

Discovery of Indazole Derivatives as a Novel Class of Bacterial Gyrase B Inhibitors

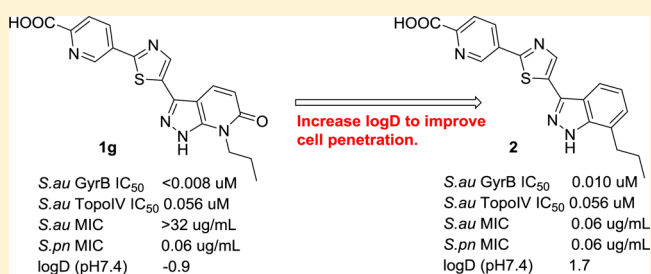
Jing Zhang,* Qingyi Yang, Jan Antoinette C. Romero, Jason Cross, Bin Wang, Katherine M. Poutsika, Felix Epie, Douglas Bevan, Yuchuan Wu, Terence Moy, Anu Daniel, Brian Chamberlain, Nicole Carter, Joseph Shotwell, Anu Arya, Vipul Kumar, Jared Silverman, Kien Nguyen, Chester A. Metcalf, III, Dominic Ryan, Blaise Lipa, and Roland E. Dolle

Cubist Pharmaceuticals Inc., Lexington, Massachusetts 02421, United States

Supporting Information

ABSTRACT: Antibacterials with a novel mechanism of action offer a great opportunity to combat widespread antimicrobial resistance. Bacterial DNA Gyrase is a clinically validated target. Through physicochemical property optimization of a pyrazolopyridone hit, a novel class of GyrB inhibitors were discovered. Guided by structure-based drug design, indazole derivatives with excellent enzymatic and antibacterial activity as well as great animal efficacy were discovered.

KEYWORDS: Antibacterial, GyrB, topoisomerase, indazole, MRSA



Because of the increasing prevalence of bacterial antibiotic resistance, the current antibiotics continue to lose their efficacy. Therefore, the investigation and development of new antibacterials that are not subject to the existing mechanisms of resistance offer a solution to this growing unmet medical need. Bacterial DNA type II topoisomerases are well-established targets. Fluoroquinolones such as ciprofloxacin act on the GyrA subunit of the DNA gyrase complex. The GyrB subunit, the target of Novobiocin, offers an opportunity for overcoming the widespread cross-resistance to fluoroquinolones. Due to the clinical success of the fluoroquinolone class of antibacterials, GyrB has attracted a great deal of interest from both industrial and academic institutions.^{1–3} Representative GyrB inhibitors are depicted in Figure 1: the tricyclic pyrimidines **1a** from Trius,⁴ aminobenzimidazoles **1b** from Vertex,^{5,6} cyclothialidines **1c** from Roche,^{7,8} pyrrolamides **1d** from Astra-Zeneca,^{9–11} imidazopyridine **1e** from Pfizer,¹² and benzothiazole **1f** from Prolysis.¹³

Based on a fragment based screen against GyrB,¹⁴ carboxylic acid-containing pyrazolopyridone **1g** was discovered and possesses potent *Staphylococcus aureus* (*Sa*) GyrB activity with an IC₅₀ < 8 nM. This excellent enzymatic activity could be explained via the X-ray crystallographic structure of an analogous compound bound in the GyrB 24kDa ATPase pocket (compound **1g** without the carboxylic acid, Figure 2, PDB code 5D7D). It engages a number of key interactions with GyrB ATP binding pocket: (1) a hydrogen bond donor–acceptor network with catalytic Asp81 and a stabilized water; (2) *N*-propyl group has favorable hydrophobic interaction within a small lipophilic pocket formed by Val79 and Ile175; (3) the distal pyridine moiety forms π –cation stacking with

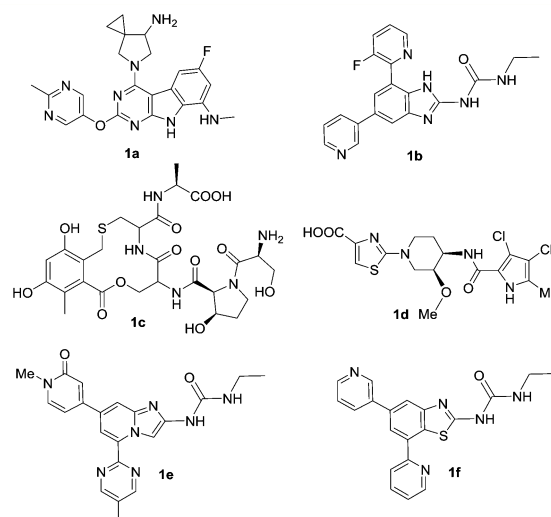


Figure 1. Representative GyrB inhibitors.

Arg84 and hydrogen bonding with Arg144 while placing the carboxylic acid in the solvent exposed region; (4) the central thiazole ring establishes hydrophobic interaction with Ile86, Ile102, and Leu10. Despite the excellent *Sa* GyrB binding potency, **1g** does not show whole cell antibacterial activity. We reasoned that the lack of MIC could be due to poor cell membrane penetration resulted from polar functional groups

Received: July 1, 2015

Accepted: September 8, 2015

Published: September 8, 2015

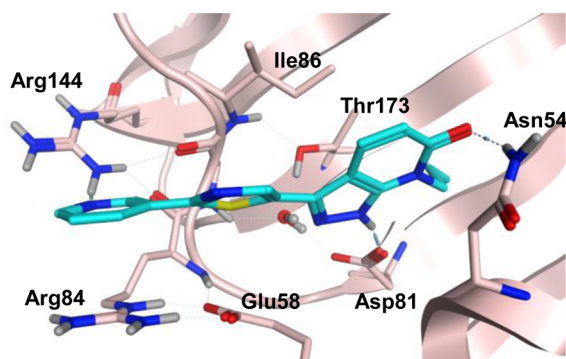


Figure 2. X-ray crystallographic structures of *S. au* GyrB ATP-binding pocket with pyrazolopyridone analogue. Protein carbons are in pink and ligand carbons are in blue.

and therefore a low logD. In an effort to improve the cell penetration for carboxylic acid-containing analogue **1g**, we decided to replace the more polar pyrazolopyridone with indazole to increase the overall logD for better cell penetration (Figure 3). Thiazolylindazoles are a well-known class of GyrB

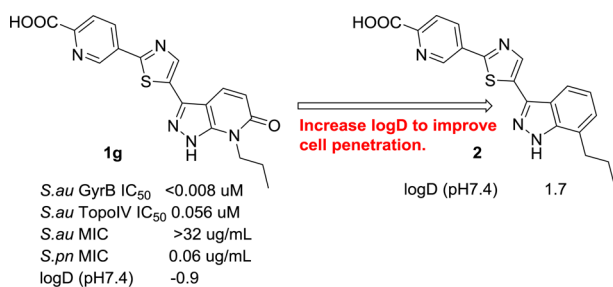
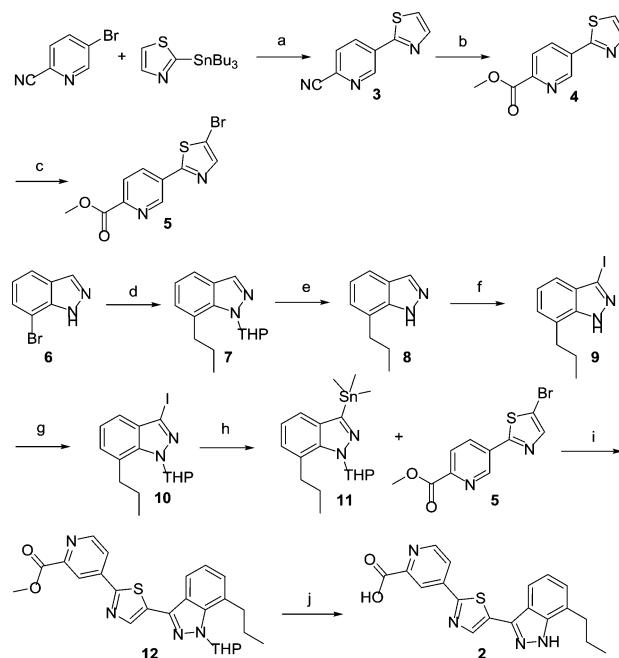


Figure 3. Indazole design strategy to improve cell penetration.

inhibitors as demonstrated by the excellent work of Roche¹⁵ and Quorex/Pfizer.¹⁶ However, only 2-thiazolylindazoles were disclosed. In our pyrazolopyridone series,¹⁴ we found that 5-thiazolyl pyrazolopyridone analogues provided ~64× better MICs than the corresponding 2-thiazolyl derivatives. Given the markedly observed MIC differences and the lack of detailed SAR disclosure from the previous works, we think that further SAR studies around the 5-thiazolylindazole scaffold are warranted.

The synthesis of **2** is outlined in Scheme 1. All indazole analogues were prepared according to this general route. The synthesis starts from commercially available 3-bromo-6-cyanopyridine and 2-tributylstannylthiazole via a standard Stille coupling to give the biaryl **3** in 82% yield. The cyanide was then unmasked with HCl in methanol to give the methyl ester **4** in 87% yield. NBS mediated bromination provide bromothiazole **5** as one of the coupling fragments. The synthesis of the other building block starts from the commercially available 7-bromoindazole **6**. THP protection followed by a standard Suzuki coupling provided intermediate **7** in 53% overall yield. We found that the yield for the Suzuki coupling was significantly better when the indazole NH was protected. Acid mediated THP deprotection gave **8** in 87% yield. Iodination of indazole **8** under strongly basic condition gave the 3-iodoindazole **9** in 75% yield. The indazole NH was reprotected in its THP form to give **10** in 65% yield. The conversion of iodoindazole to the trimethylstannane **11** provided the other building block. The key Stille coupling

Scheme 1. Synthesis of Indazoles^a

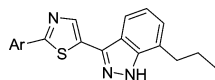


^aReagents and conditions: (a) Pd(PPh₃)₂Cl₂, 1,4-dioxane, 110 °C, 82%; (b) 4 M HCl in dioxane, MeOH, 75 °C, 87%; (c) NBS, acetonitrile, 90 °C, 78%; (d) 1. dihydropyran, TFA, 90 °C; 2. *n*-PrB(OH)₂, Pd(dppf)Cl₂, aq. Na₂CO₃, 1,4-dioxane, 110 °C, 53%; (e) TFA, DCM, RT, 87%; (f) KOH, I₂, RT, 75%; (g) dihydropyran, TFA, 90 °C, 65%; (h) Pd(PPh₃)₂Cl₂, Me₆Sn₂, 1,4-dioxane, 100 °C, 65%; (i) Pd(PPh₃)₂Cl₂, P(furyl)₃, 1,4-dioxane, 100 °C, 52%; (j) 6 M aq HCl, 100 °C, 76%.

between **5** and **11** proceeded uneventfully to give **12** in 52% yield, which underwent THP deprotection under acidic conditions to provide the target compound **2** in 76% yield after purification.

Biological testing showed that **2** possessed an excellent Gram positive MIC profile in addition to retaining enzymatic activity (Table 1), therefore validating our hypothesis that increased logD over pyrazolopyridone analogue **1g** would improve cell penetration. Based on the SAR knowledge gained from our previous pyrazolopyridone series, our efforts toward optimizing this class as potent Gram positive antibacterial agent were focused on physicochemical property exploration and further target binding affinity optimization. Specifically, our goals were to (1) optimize the interactions with Arg84 and Arg144 with different left-hand heterocycles; (2) tune the physicochemical properties via attaching solubilizing groups off the aforementioned heterocycles; (3) explore indazole phenyl ring SAR to enhance binding affinity.

The SAR around the left-hand heteroaryl is summarized in Table 1. Methyl ester **13** shows a much worse MIC profile than **2**, due to weaker GyrB and Topo IV binding. Hydroxymethyl analogue **14** gives a similar IC₅₀ for GyrB; however, it is much weaker against TopoIV. It maintains the excellent level of MICs for *Sa* while compromising those for *Streptococcus pneumoniae* (*Spn*) and *Enterococcus faecium* (*Ef*). Because of **14**'s superb *Sa* MICs and poor aqueous solubility, its phosphate prodrug **15** was prepared. Interestingly, **15** shows a reasonable MIC profile with much improved MICs vs *Spn* and *Ef*.¹⁸ As a representative example of the amides we prepared, **16** shows weaker IC₅₀s and MICs, demonstrating the important contribution of the salt

Table 1. Optimization of Interactions with Arginine Residues: Left-Hand Aryl Group SAR^a

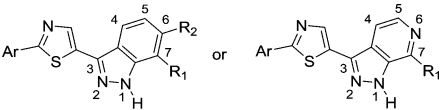
Compd	Ar	<i>Sa</i> GyrB ATPase IC ₅₀ (μ M) ^b	<i>Sa</i> TopoIV ATPase IC ₅₀ (μ M)	MICs (μ g/mL)					
				<i>Sa</i> 42 MSSA	<i>Sa</i> 1118 MRSA	<i>Sa</i> 1721 MRSA Cipro ^R	<i>S.</i> <i>pneum</i>	<i>E.</i> <i>faecium</i>	<i>E.</i> <i>faecalis</i>
2		0.010	0.056	0.06	0.06	0.06	0.06	0.06	0.03
13		0.029	>10	0.5	1	2	0.125	>8	>8
14		0.015	>4	0.06	0.06	0.06	8	>8	>8
15		0.009	0.147	0.25	0.25	0.50	2	2	>8
16		0.020	>2	2	1	2	>8	>8	>8
17		0.025	0.434	0.25	0.25	0.25	0.5	4	0.5
18		0.011	>1	>8	>8	>8	1	>8	>8
19		0.049	9.9	8	>8	>8	8	4	8
20		0.014	0.115	1	1	>8	1	4	2
21		<0.008	0.024	0.125	0.125	0.25	0.25	0.25	0.25
22		<0.008	1.3	0.125	0.125	0.125	0.25	0.06	0.06
23		0.011	0.060	0.125	0.06	0.125	0.5	0.125	0.125
24		<0.008	0.068	1	1	2	1	2	1
25		0.168	NA	>8	>8	>8	>8	>8	>8
26		0.012	0.06	0.02	0.02	0.03	0.125	0.013	0.06
27	H	6.50	NA	>32	>32	>32	>32	>32	>32

^aNA = not determined. ^bOur GyrB IC₅₀ assay detection limit is ~10 nM. A more accurate assay was developed later.¹⁷

bridge interaction between the carboxylic acid of **2** and Arg144 toward enzymatic activity. However, pyridine acetic acid analogue **17** has an 8 \times loss in TopoIV IC₅₀ while displaying 4–8 \times weaker MICs. Moving the pyridine nitrogen atom or carboxylic acid around the ring leads to diminished GyrB inhibitions (**18** and **19**). These data suggest that both the rigidity and the bidentate hydrogen bond or salt bridge interaction with Arg144 are critical for GyrB inhibition and whole cell activity. Efforts to better engage Arg144 through an additional hydrogen bond acceptor such as *m*-F, OH, and OMe resulted in the syntheses of **20–24**. All of these compounds

give potent GyrB and TopoIV IC₅₀s and slightly weaker MIC profile than **2**. Fluorobenzoic acid analogue **22** is especially interesting due to its much improved aqueous solubility¹⁹ and excellent overall MIC profile. The carboxyl pyridone analogue **25** gives poor enzymatic activity and MICs. The *o*-Me analogue **26** was designed to increase the aqueous solubility by disrupting the coplanarity of the left-hand biaryl. Though it shows similar IC₅₀s, its MICs are improved several folds in all the *Sa* strains and an *Ef* strain. Lastly, to gauge how much the left-hand carboxypyridine contributes to the overall enzyme

Table 2. Indazole Ring Substitution SAR



Compd	Ar	R ₁	R ₂	<i>Sa</i> GyrB ATPase IC ₅₀ (μ M) ^a	MICs (μ g/mL)					
					<i>Sa</i> 42 MSSA	<i>Sa</i> 1118 MRSA	<i>Sa</i> 1721 MRSA Cipro ^R	<i>S.</i> <i>pneum</i>	<i>E.</i> <i>faecium</i>	<i>E.</i> <i>faecalis</i>
2		n-propyl	H	<0.008	0.06	0.06	0.06	0.06	0.06	0.03
28		n-propyl	-OH	0.013	1	4	2	0.25	0.25	0.125
29		n-propyl	-OH	0.008	0.125	0.125	0.125	0.06	0.25	0.06
30		n-propyl	-OH	0.011	0.125	0.25	0.25	0.06	0.02	0.02
31		n-propyl	-OMe	0.015	0.06	0.125	0.125	0.125	0.03	0.03
32			H	0.009	0.03	0.03	0.06	0.25	0.125	0.125
33			H	0.013	0.05	0.05	0.10	0.5	4	0.125
34			H	<0.008	0.5	0.5	1	1	2	1
35			Azaindazole	<0.008	0.25	0.5	0.5	0.125	0.5	0.25
36		n-propyl	Azaindazole	0.052	8	8	8	0.125	8	4
37		n-propyl	Azaindazole	<0.008	4	4	8	0.06	2	2
38		n-propyl	Azaindazole	<0.008	0.125	0.25	0.125	0.25	1	0.25
39		n-propyl	Azaindazole	<0.008	8	8	>8	1	8	>8

^aOur GyrB IC₅₀ assay detection limit is ~10 nM. A more accurate assay was developed later.¹⁷

affinity, the des-pyridine analogue **27** was prepared and only shows a 6.5 μ M GyrB IC₅₀ and no measurable MICs.

The limited antibacterial activity improvements through the left-hand heteroaryl modifications indicate that the carboxypyridine motif is already fairly optimal in terms of engaging Arg84 and Arg144, though several analogues show improvements in the overall physicochemical properties relative to **2**. We next turned our attention to the indazole core region to improve the enzymatic and antibacterial activity. Based on our previous SAR in the pyrazolopyridone series,¹⁴ we chose to focus our efforts on C6 and C7 positions of the indazole core while leaving out C4 and C5. The C6 and C7 SAR is detailed in Table 2.

At the corresponding C6 position of pyrazolopyridone **1g**, there is a pyridone carbonyl that forms a hydrogen bond with Asn54 (Figure 2). Trius also reported that engaging this Asn54 was critical for the enhanced enzymatic and antibacterial

activities of their tricyclic GyrB inhibitors.²⁰ In an effort to re-engage Asn54 with the indazole nucleus, we designed 6-OH and 6-OMe 7-*n*-propylindazole, then combined them with a few best left-hand fragments and prepared analogues **28–31**. We were able to resolve the crystal structure of **28** bound in the 24 kDa GyrB active site (Figure 4, PDB code 5D7R). In addition to the contacts observed with our previous pyrazolopyridone series, the crystal structure confirms that (1) the pyridine acid motif is engaged in a bidentate hydrogen bond interaction with Arg144 through both the carboxylic acid oxygen and pyridine nitrogen; (2) the hydroxyl group on the pyridine ring points to the solvent, and the π -cation interaction with Arg84 is also maintained; (3) the 6-hydroxyl group on the indazole ring indeed makes a hydrogen bond interaction with Asn54. It is hard to conclude if this newly formed hydrogen bond leads to improved binding affinity as

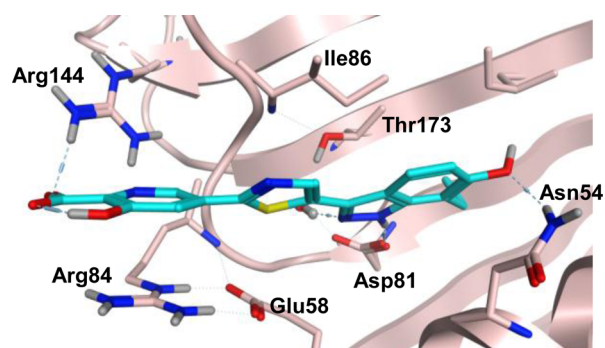


Figure 4. X-ray crystallographic structure of compound **28** bound in *Sa* GyrB ATPase binding pocket. Protein carbons are in brown, and ligand carbons are in blue.

they all have IC_{50} s below our assay detection limits. Compounds **28** and **29** show slightly worse MICs than the C6 unsubstituted analogues **23** and **26**, while fluorobenzoic acid analogues **30** and **31** display similar *Sa* and *Spn* MICs and superior *Ef* and *Em* MICs compared to **22**.

As shown in Figure 4,²¹ the C7 *n*-propyl group directly points toward the small hydrophobic pocket formed by Val79 and Ile175. This lipophilic interaction is critical for GyrB binding affinity just like the pyridone *N*-propyl substituent. Among the analogues prepared, only C7 allyl analogue **32** gives a similar MIC profile to **2**. Other analogues such as **33** and **34** have much weaker MICs than their corresponding *n*-propyl parents. A few 6-azaindazole derivatives **35**–**39** were also prepared in order to fine-tune the overall physicochemical properties with the expectation that the N6 of azaindazole is too far from Asn54 to make hydrogen bond contact. Though none of them gives better MIC profile than **2**, **35** and **38** still possess impressive Gram positive MICs. To improve the solubility of **38** for IV delivery, the phosphate prodrug **39** was prepared, which had an aqueous solubility of >25 mg/mL.

A few selected compounds were progressed into mouse *in vivo* PK and efficacy studies, and the results are depicted in Table 3. Compound **2** shows impressive *Sa* septicemia efficacy with a mice protection PD_{50} of 1 mg/kg. Unfortunately, it does not show appreciable level of *Spn* lung efficacy due to the poor lung permeability and the solubility limitation, and possibly high clearance resulted from the indazole NH glucuronidation.²² Benzoic acid analogues **22** and **31** show similarly moderate levels of *Spn* lung efficacy. Though **31** displays slightly better *Spn* MIC and mouse exposure, it probably has poorer tissue penetration relative to **22**, resulting in similar lung efficacy.

In summary, the indazole class of GyrB inhibitors, derived from the pyrazolopyridone series and guided by structure-based drug design and physicochemical properties optimization,

showed both excellent enzymatic and antibacterial activity against clinically important Gram-positive pathogens including MRSA, fluoroquinolone resistant MRSA, *Streptococcus pneumoniae*, *Enterococcus faecium*, and *Enterococcus faecalis*. As a result of their excellent antibacterial activity and favorable PK properties, good animal efficacy was observed in various mouse infection models for selected compounds. Further preclinical evaluation of the indazole class of GyrB inhibitors is ongoing and will be reported in due course.

■ ASSOCIATED CONTENT

📄 Supporting Information

The Supporting Information is available free of charge on the ACS Publications website at DOI: 10.1021/acsmchemlett.5b00266.

Experimental procedure for the synthesis of **2**, the general procedure for GyrB and TopoIV IC_{50} determination, MIC protocol, X-ray crystal structure determination, an alternative view of **28**/GyrB cocrystal structure, mouse septicemia and lung efficacy procedure, and a general PK protocol (PDF)

■ AUTHOR INFORMATION

Corresponding Author

*E-mail: jackzhang49@yahoo.com. Phone: (781) 640-2333.

Notes

The authors declare no competing financial interest.

■ ACKNOWLEDGMENTS

We would like to thank Dr. Ole Andersen and Dr. John Barker at Evotec AG for the crystallographic work, and Dr. Hongwu Gao's team in Chempartner for analogue synthesis.

■ ABBREVIATIONS

ADME, absorption, distribution, metabolism, and excretion; DCM, dichloromethane; dppf, diphenylphosphinoferrocene; *Ef*, *Enterococcus faecalis*; *Em*, *Enterococcus faecium*; GyrA, gyrase A; GyrB, gyrase B; MIC, minimum inhibitory concentration; MRSA, methicillin-resistant *Staphylococcus aureus*; MSSA, methicillin-susceptible *Staphylococcus aureus*; NBS, *N*-bromosuccinimide; PK, pharmacokinetics; SAR, structure–activity relationship; *Sa*, *Staphylococcus aureus*; *Spn*, *Streptococcus pneumoniae*; TFA, trifluoroacetic acid; THP, tetrahydropyran; Topo IV, topoisomerase IV

■ REFERENCES

(1) Tomašić, T.; Mašič, L. P. Prospects for developing new antibacterials targeting bacterial type IIA topoisomerases. *Curr. Top. Med. Chem.* **2014**, *14* (1), 130–51.

Table 3. Mice *in Vivo* Efficacy and IV PK

compd	<i>Sa</i> 1118 MIC (μ g/mL)	septicemia efficacy PD_{50} (mg/kg)	<i>Spn</i> MIC (μ g/mL)	lung efficacy ED_{2log}/ED_{3log} (mg/kg)	DNAUC ^a (μ g·h/mL)/(mg/kg)	V _{dss} (L/kg)	$t_{1/2}$ (h)	Cl (mL/min/kg)
Novobiocin	0.125	10	2	>100/>100	ND	ND	ND	ND
2	0.06	1	0.06	>25/>25 ^c	0.159	3.47	2.1	105
22	0.125	ND ^b	0.25	63.0/97.6	0.397	1.70	2.0	42
31	0.125	ND	0.125	60.6/103.7	0.893	0.32	0.31	19
Moxifloxacin	ND	ND	0.06	28.6/50.8	ND	ND	ND	ND

^aMice were dosed IV at 2 mg/kg. ^bNot determined. ^cThe highest achievable IV dose due to the solubility limitation.

- (2) Oblak, M.; Kotnik, M.; Solmajer, T. Discovery and development of ATPase inhibitors of DNA gyrase as antibacterial agents. *Curr. Med. Chem.* **2007**, *14* (19), 2033–47.
- (3) Collin, F.; Karkare, S.; Maxwell, A. Exploiting bacterial DNA gyrase as a drug target: current state and perspectives. *Appl. Microbiol. Biotechnol.* **2011**, *92* (3), 479–497.
- (4) Tari, L. W.; Li, X.; Trzoss, M.; Bensen, D. C.; Chen, Z.; Lam, T.; Zhang, J.; Lee, S. J.; Hough, G.; Phillipson, D.; Akers-Rodriguez, S.; Cunningham, M. L.; Kwan, B. P.; Nelson, K. J.; Castellano, A.; Locke, J. B.; Brown-Driver, V.; Murphy, T. M.; Ong, V. S.; Pillar, C. M.; Shinabarger, D. L.; Nix, J.; Lightstone, F. C.; Wong, S. E.; Nguyen, T. B.; Shaw, K. J.; Finn, J. Tricyclic GyrB/ParE (TriBE) inhibitors: a new class of broad-spectrum dual-targeting antibacterial agents. *PLoS One* **2013**, *8* (12), 1–13.
- (5) Ronkin, S. M.; Badia, M.; Bellon, S.; Grillot, A. L.; Gross, C. H.; Grossman, T. H.; Mani, N.; Parsons, J. D.; Stamos, D.; Trudeau, M.; Wei, Y.; Charifson, P. S. Discovery of pyrazolthiazoles as novel and potent inhibitors of bacterial gyrase. *Bioorg. Med. Chem. Lett.* **2010**, *20*, 2828–2831.
- (6) Charifson, P. S.; Grillot, A.-L.; Grossman, T. H.; Parsons, J. D.; Badia, M.; Bellon, S.; Deininger, D. D.; Drumm, J. E.; Gross, C. H.; LeTiran, A.; Liao, Y.; Mani, N.; Nicolau, D. P.; Perola, E.; Ronkin, S.; Shannon, D.; Swenson, L. L.; Tang, Q.; Tessier, P. R.; Tian, S.-K.; Trudeau, M.; Wang, T.; Wei, Y.; Zhang, H.; Stamos, D. Novel dual-targeting benzimidazole urea inhibitors of DNA gyrase and topoisomerase IV possessing potent antibacterial activity: intelligent design and evolution through the judicious use of structure-guided design and structure-activity relationships. *J. Med. Chem.* **2008**, *51* (17), 5243–63.
- (7) Lewis, R. J.; Singh, O. M.; Smith, C. V.; Skarzynski, T.; Maxwell, A.; Wonacott, A. J.; Wigley, D. B. The nature of inhibition of DNA gyrase by the coumarins and the cyclothialidines revealed by X-ray crystallography. *EMBO J.* **1996**, *15*, 1412–1420.
- (8) Angehrn, P.; Goetschi, E.; Gmuender, H.; Hebeisen, P.; Hennig, M.; Kuhn, B.; Luebbers, T.; Reindl, P.; Ricklin, F.; Schmitt-Hoffmann, A. A new DNA gyrase inhibitor subclass of the cyclothialidine family based on a bicyclic dilactam-lactone scaffold. Synthesis and antibacterial properties. *J. Med. Chem.* **2011**, *54* (7), 2207–24.
- (9) Dumas, J.; Sherer, B. (2-Pyridin-3-ylimidazo[1,2-b]pyridazin-6-yl) urea derivatives as antibacterial agents. Int. Pat. Appl. WO2009027733 A1.
- (10) Basarab, G.; Hill, P.; Zhou, F. Piperidine compounds and uses thereof. Int. Pat. Appl. WO2008152418 A1.
- (11) Illingworth, R. N.; Uria-Nickelsen, M.; Bryant, J.; Eakin, A. E. Presented at the 48th Interscience Conference on Antimicrobial Agents and Chemotherapy (ICAAC), 2008, Poster F1-2028.
- (12) Starr, J. T.; Sciotti, R. J.; Hanna, D. L.; Huband, M. D.; Mullins, L. M.; Cai, H.; Gage, J. W.; Lockard, M.; Rauckhorst, M. R.; Owen, R. M.; Lall, M. S.; Tomilo, M.; Chen, H.; McCurdy, S. P.; Barbachyn, M. R. 5-(2-Pyrimidinyl)-imidazo[1,2-a]pyridines are antibacterial agents targeting the ATPase domains of DNA gyrase and topoisomerase IV. *Bioorg. Med. Chem. Lett.* **2009**, *19* (18), 5302–06.
- (13) Haydon, D. R.; Czaplowski, L. G.; Palmer, N. J.; Mitchell, D. R.; Atherall, J. F.; Steele, C. R.; Ladduwahetty, T. Antibacterial compositions. Int. Pat. Appl. WO2007148093 A1.
- (14) The fragment based GyrB inhibitors will be published in a separate communication.
- (15) Boehm, H.; Boehringer, M.; Bur, D.; Gmuender, H.; Huber, W.; Klaus, W.; Kostrewa, D.; Kuehne, H.; Luebbers, T.; Meunier-Keller, N.; Mueller, F. Novel Inhibitors of DNA Gyrase: 3D Structure Based Biased Needle Screening, Hit Validation by Biophysical Methods, and 3D Guided Optimization. A Promising Alternative to Random Screening. *J. Med. Chem.* **2000**, *43*, 2664–74.
- (16) Yager, K.; Chu, S.; Appelt, K.; Li, X. Preparation of thiazolylindazoles as inhibitors of bacterial DNA gyrase B inhibitors. US20050054697 A1.
- (17) Unpublished results.
- (18) Prodrug was found to be stable in the MIC assay media.
- (19) A complete disclosure of the physicochemical and ADME properties of the indazole derivatives will be reported in a future full paper.
- (20) Li, X.; Tari, L. W.; Bensen, D. C.; Trzoss, M.; Lam, T.; Zhang, J.; Chen, Z.; Lee, S.-J.; Cunningham, M.; Kwan, B.; Nelson, K.; Stidham, M.; Brown-Driver, V.; Hough, G.; Phillipson, D.; Nguyen, T.; Lightstone, F.; Wong, S.; Shaw, K. J.; Finn, J. Presented at the 52nd Interscience Conference on Antimicrobial Agents and Chemotherapy (ICCAC), 2012, Poster F-2017.
- (21) An alternative view of the X-ray structure was included in the [Supporting Information](#).
- (22) Rose, K.; Yang, Y.; Sciotti, R.; Cai, H. Structure-activity relationship (SAR): effort towards blocking N-glucuronidation of indazoles (PF-03376056) by human UGT1A enzymes. *Drug Metab. Lett.* **2009**, *3*, 28–34.